Supplementary information for

Identification of highly selective covalent inhibitors by phage display

Shiyu Chen[1], Scott D. Lovell[1], Sumin Lee[1], Matthias Fellner[3], Peter D. Mace[3] and Matthew S. Bogyo[1,2]*

[1] Department of Pathology and [2] Department of Microbiology and Immunology, Stanford University School of Medicine, Stanford, CA 94305, USA. [3] Biochemistry Department, School of Biomedical Sciences, University of Otago, P.O. Box 56, 710 Cumberland St., Dunedin 9054, New Zealand

*E-mail: mbogyo@stanford.edu

Telephone: +1 (650) 725-4132

Fax: +1 (650) 725-7424

Supplementary Figures

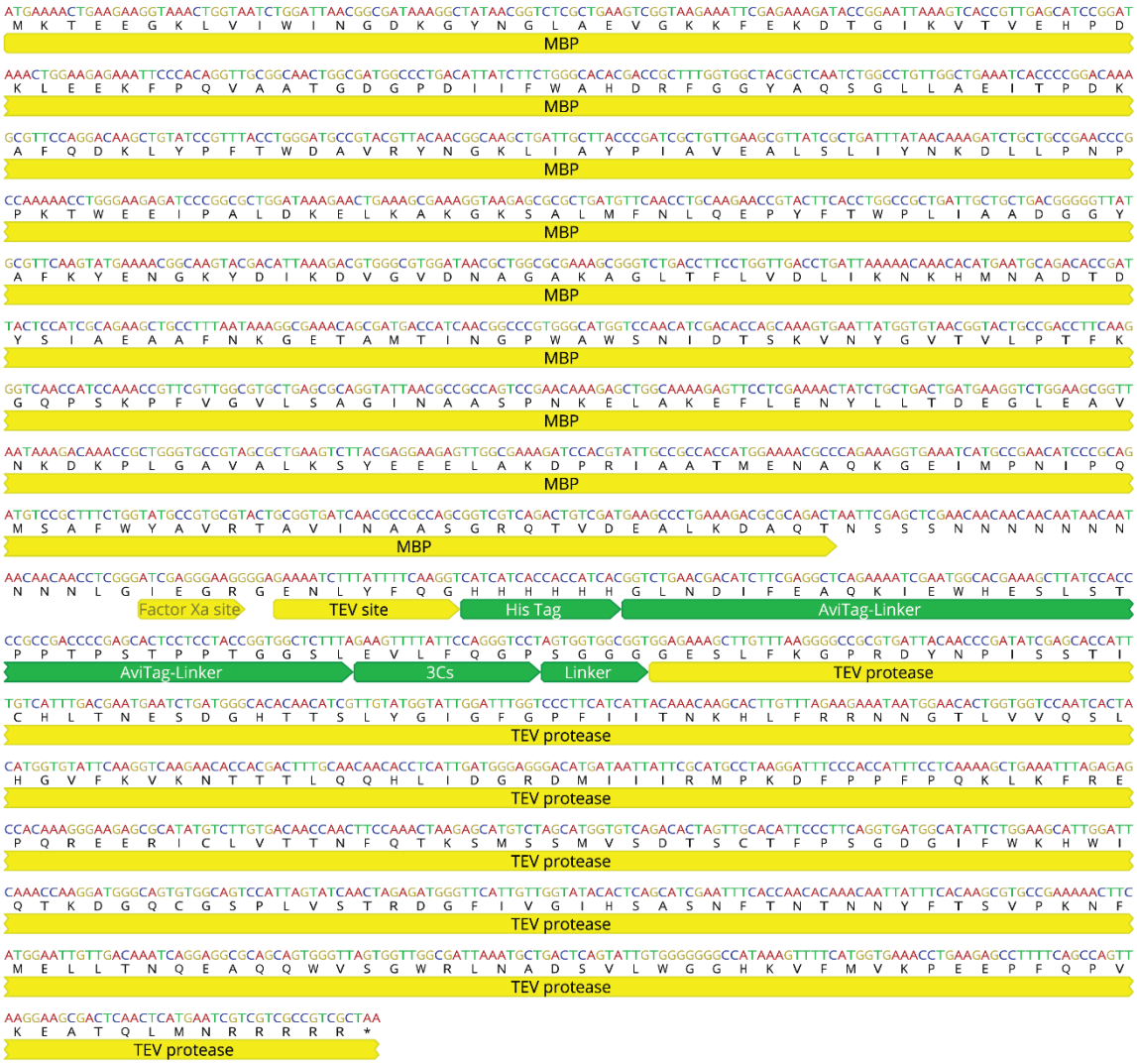

Supplementary Figure 1. Expression construct for producing biotinylated TEV protease using the AviTag. The bacteria expression vector is built on the pMalC2 backbone. To improve the solubility of TEV protease in the cytosol of the expression host, an MBP domain is fused at the N-terminus of the expression construct. A TEV protease auto-cleavable peptide sequence (ENLYFQ|G) is placed before the expected TEV protease to allow the removal of MBP after translation. The desired TEV protease domain is N-terminally conjugated with a HisTag (for affinity purification), a Biotin AviTag (for immobilizing TEV protease on solid support), a rigid proline linker (to improve BirA biotinylation efficiency), a 3C protease cutting sequence (to allow orthogonally release TEV protease from solid support with 3C protease) and a flexible linker (to achieve efficient release TEV protease from solid support with 3C protease). Data Availability at GenBank accession numbers 2264028.

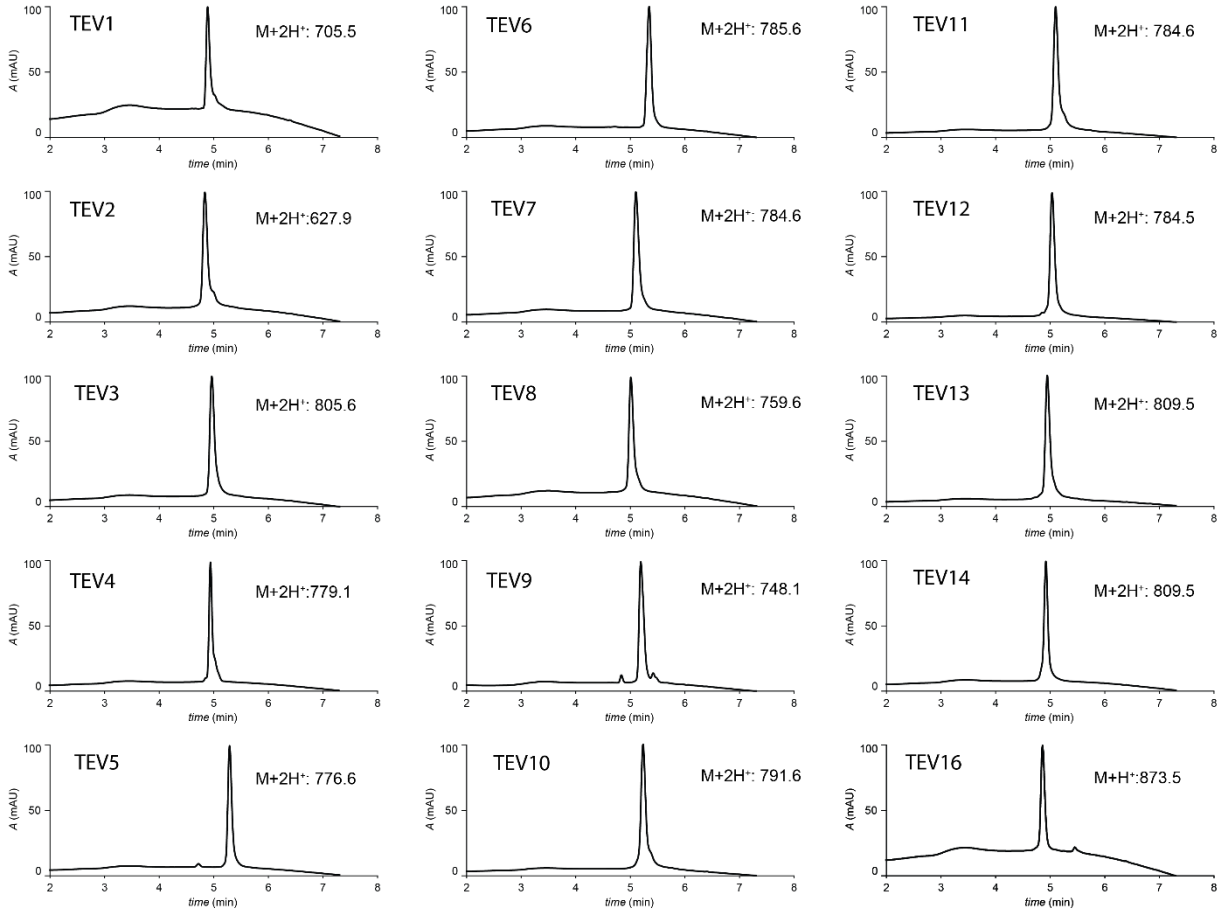

Supplementary Figure 2. HPLC analysis of the vinyl sulfone cyclic peptides listed in Fig. 3b-d. For analysis, 1 µL of 3 mM peptide stock solutions were injected into an Agilent 1260 Infinity HPLC system. Spectra of the absorbance at a wavelength of 220 nm and observed ESI MS of the corresponding peaks are shown.

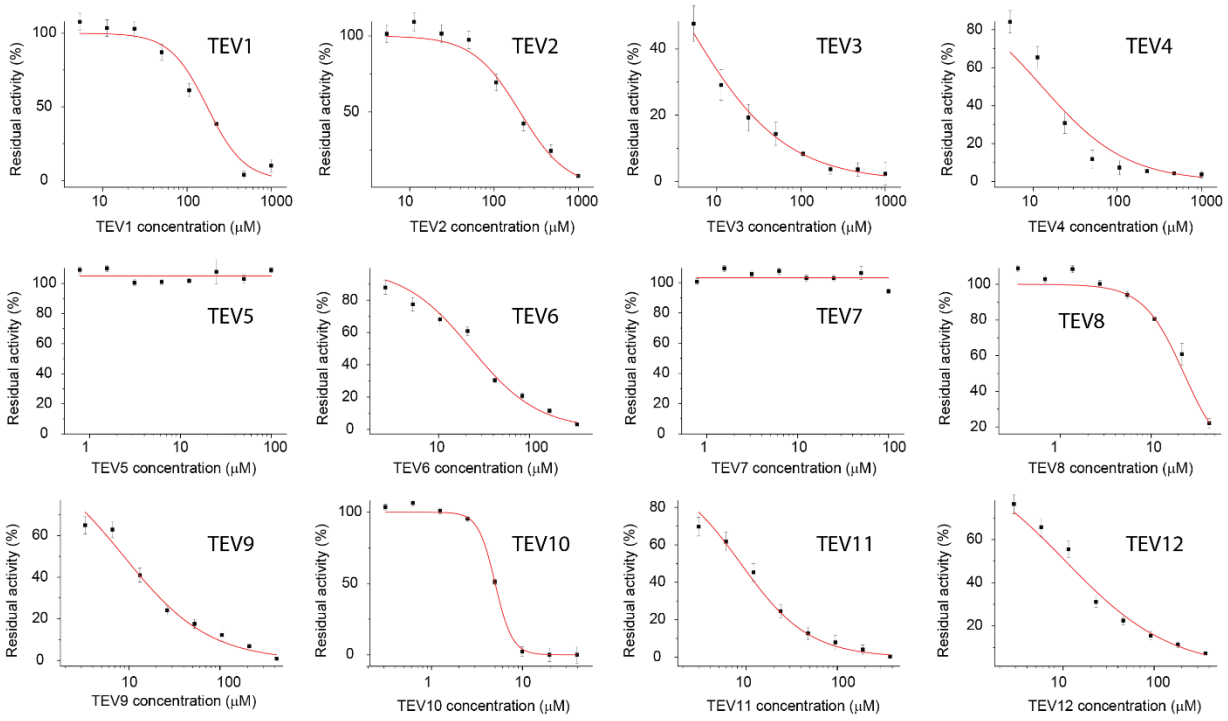

Supplementary Figure 3. Dose response inhibition studies of the cyclized peptides TEV1 to TEV12 from Fig. 4 using recombinant TEV. Plots show residual enzyme activity over a range of inhibitor doses as measured by hydrolysis of a fluorogenic substrate. Enzyme was pre-treated with inhibitor at the indicated concentrations for 1 hour followed by addition of substrate and measurement of activity.

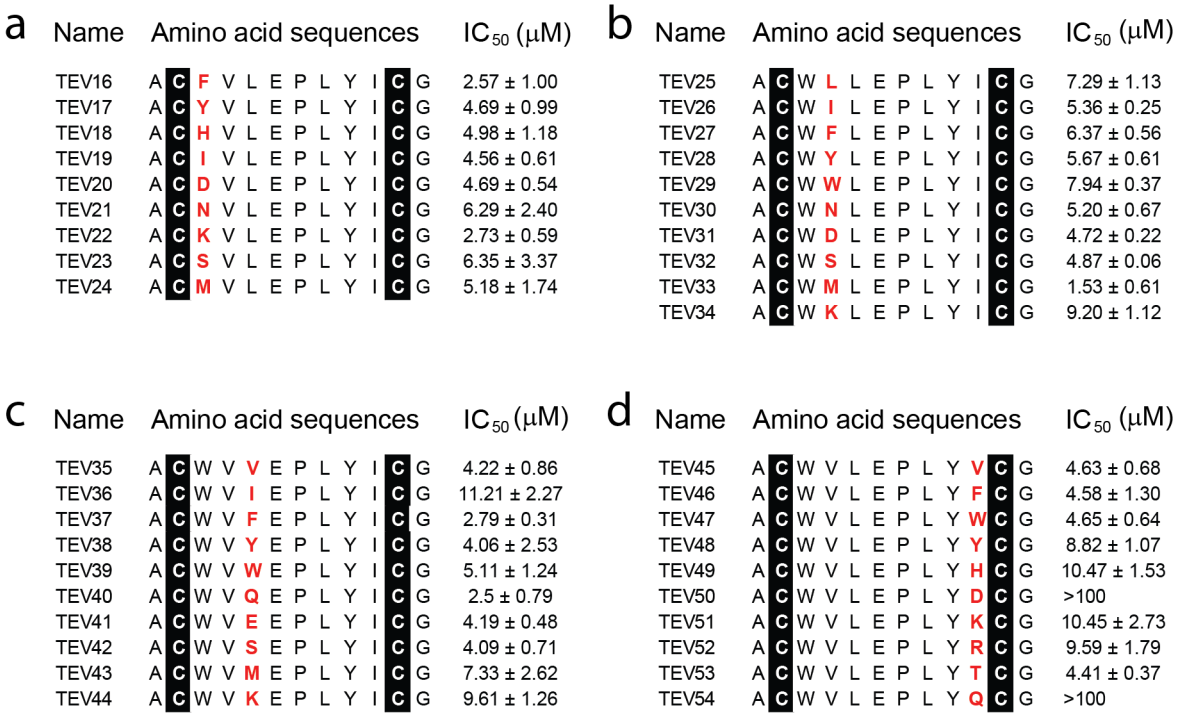

Supplementary Figure 4. Sequence activity relationship (SAR) study of cyclic peptide TEV3 by mutating residues at position (a) 3, (b) 4, (c) 5 and (d) 10 with amino acids of different properties of hydrophobicity, charge and size. The potency of each corresponding cyclic peptide-VS for TEV protease is listed to the right as an IC_{50} value.

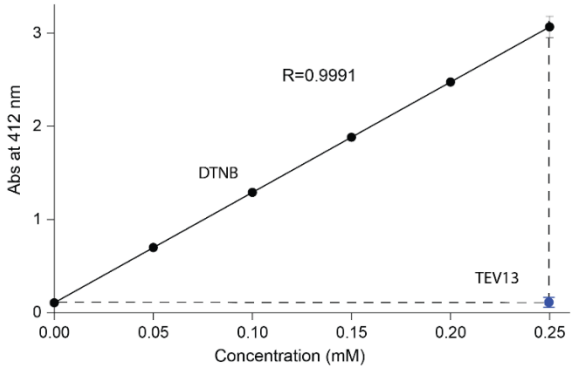

Supplementary Figure 5. Ellman's test to determine the extent of unmodified cysteine on the cyclic peptide ABP TEV13. According to the standard curve generated using free cysteine, no significant amount of free thiol is present in 0.25 mM cyclized peptide TEV13.

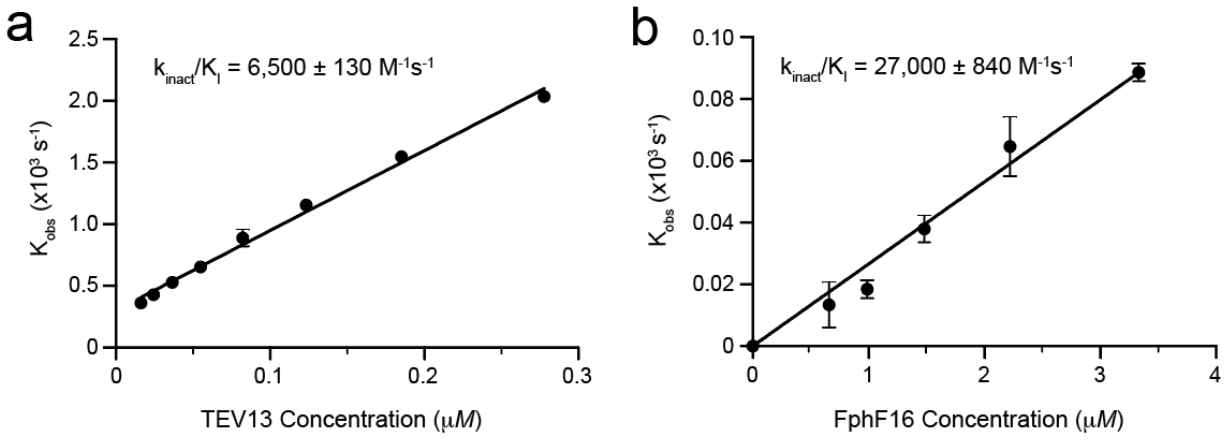

Supplementary Figure 6. Quantitative determination of irreversible inhibitor potencies through an endpoint binding assay. The time-dependent inactivation potency ratio k_{inact}/K_I values were calculated for (a) TEV13 using TEV protease and (b) FphF16 using FphF hydrolase.

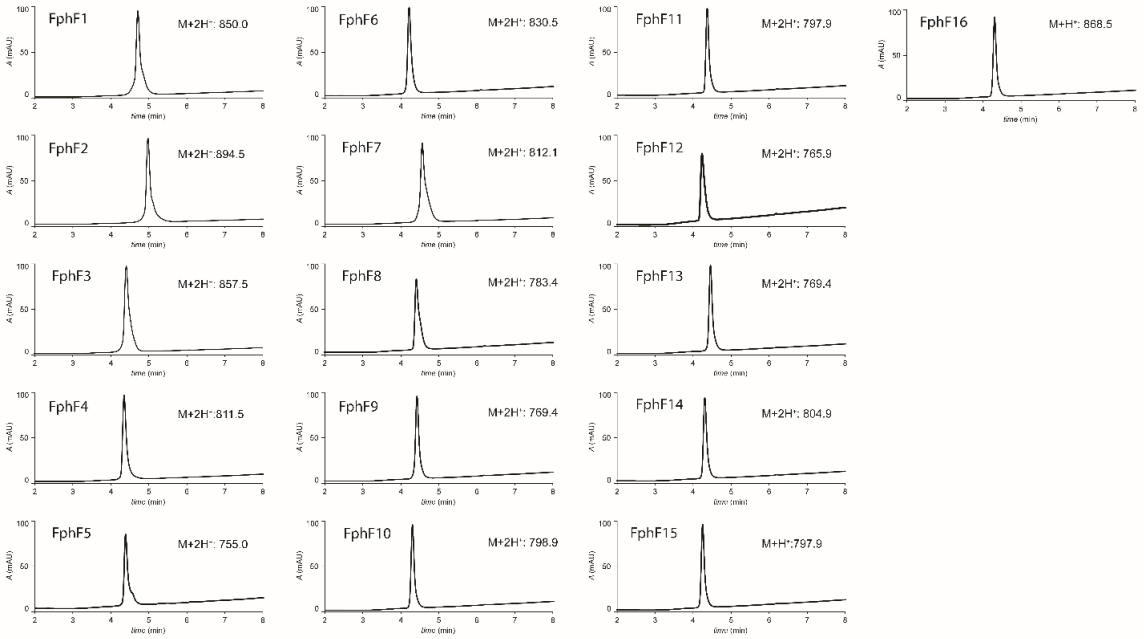

Supplementary Figure 7. HPLC analysis of diphenylphosphonate cyclic peptides from Fig. 3f-h. For analysis 1 μL of 3 mM peptide stock solutions were injected into an Agilent 1260 Infinity HPLC system. Spectra of the absorbance at a wavelength of 220 nm and observed ESI MS of the corresponding peaks are presented.

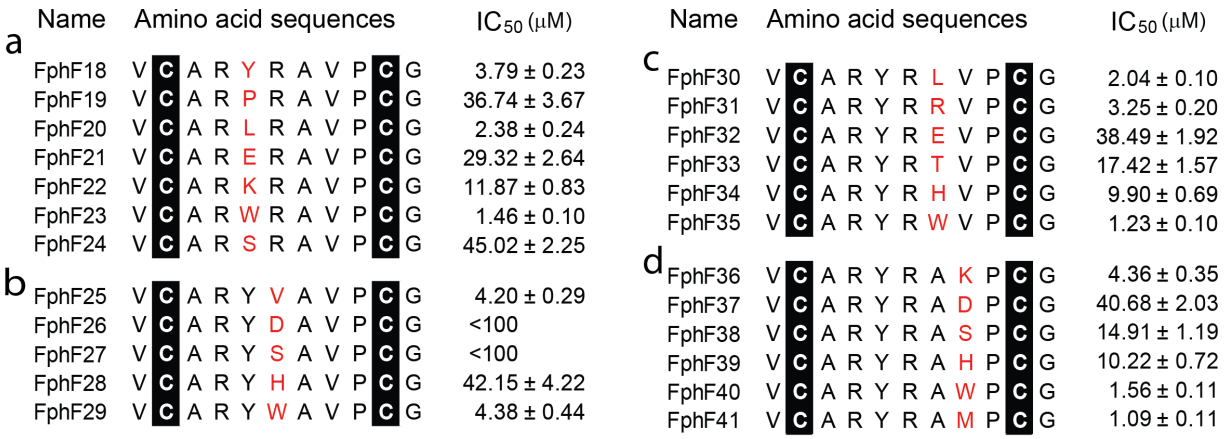

Supplementary Figure 8. Sequence activity relationship (SAR) study of cyclic peptides targeting FphF. Peptides were synthesized by mutating residues at position (a) 4, (b) 5, (c) 6 and (d) 7 with amino acids of different properties of hydrophobicity, charge and size. The potency the resulting cyclic peptide-DPPs for FphF hydrolase is listed to the right as an IC_{50} value.

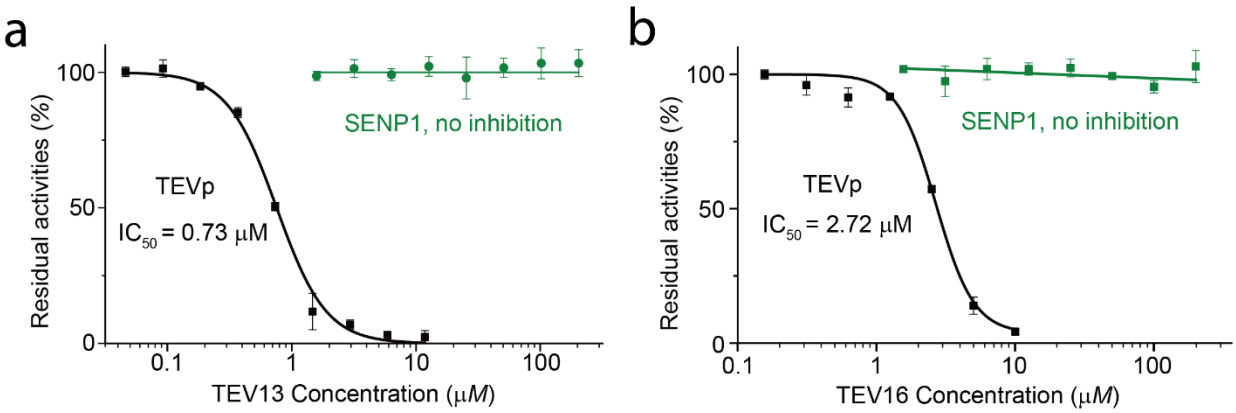

Supplementary Figure 9. Cyclic peptide TEV13 and linear peptide TEV16 inhibit TEV protease but not SENP1. Inhibition curves are shown for TEV13 left and TEV16 right for TEV protease and recombinant SENP1.

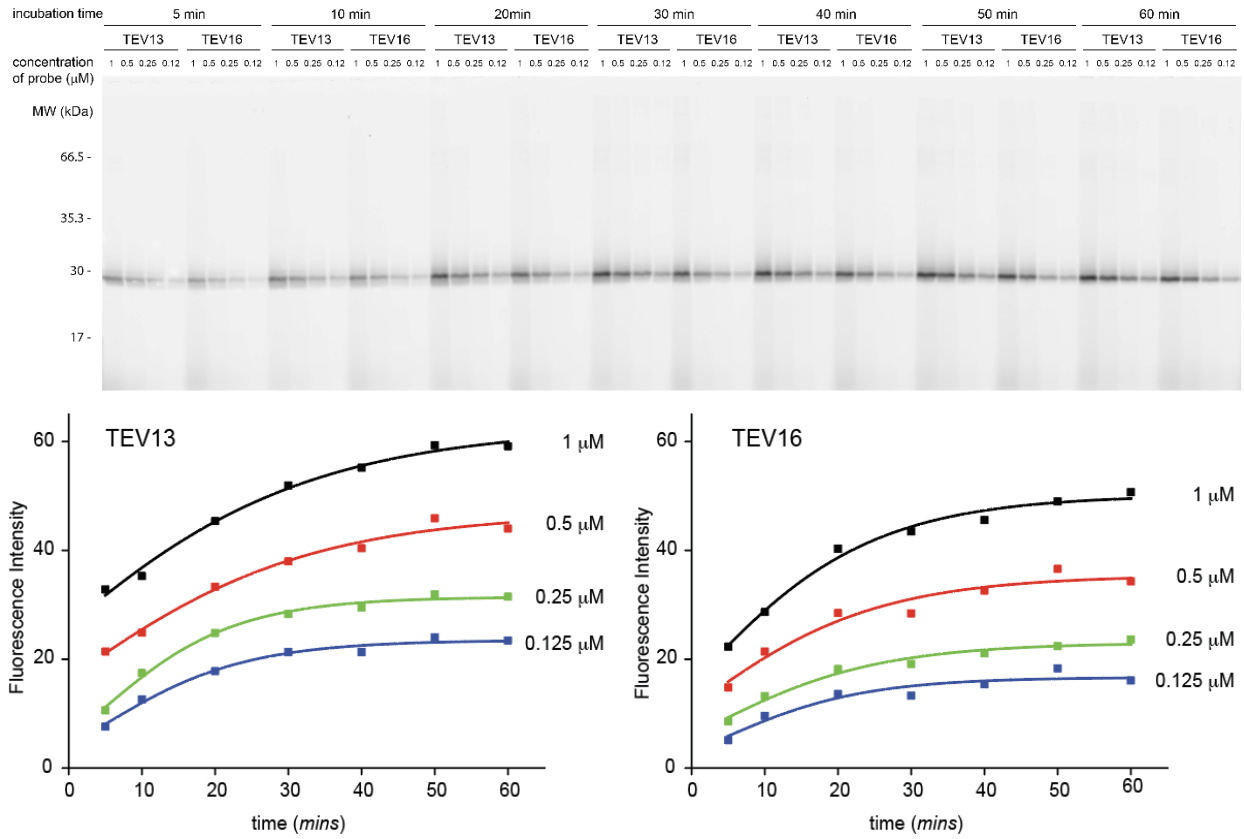

Supplementary Figure 10. Labeling of TEV protease by fluorescently labeled cyclic peptide probe TEV13 and linear peptide probe TEV16 confirms that TEV13 is a faster and more efficient label of TEV protease. TEV protease (100 nM) was incubated with increasing concentrations of the indicated fluorescent probes at 30 °C for the indicated times. After stopping the labeling reactions by adding SDS PAGE gel sample buffer and boiling, the labeling mixtures were analyzed by gel electrophoresis and detected by fluorescent scanning with a Typhoon flatbed fluorescent scanner using the Cy5 channel. The fluorescence intensity of Cy5-labeled TEV protease was determined and plotted (bottom).

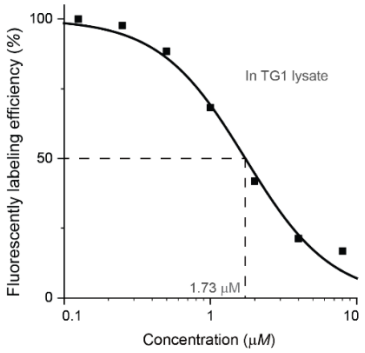

Supplementary Figure 11. Competition of Cy5-TEV13 labeling of TEV protease by TEV13 in TG1 cell lysates. Plot shows values for the percent residual labeling by Cy5-TEV13 at the indicated TEV13 concentrations. The resulting IC_{50} for inhibition of labeling is shown.

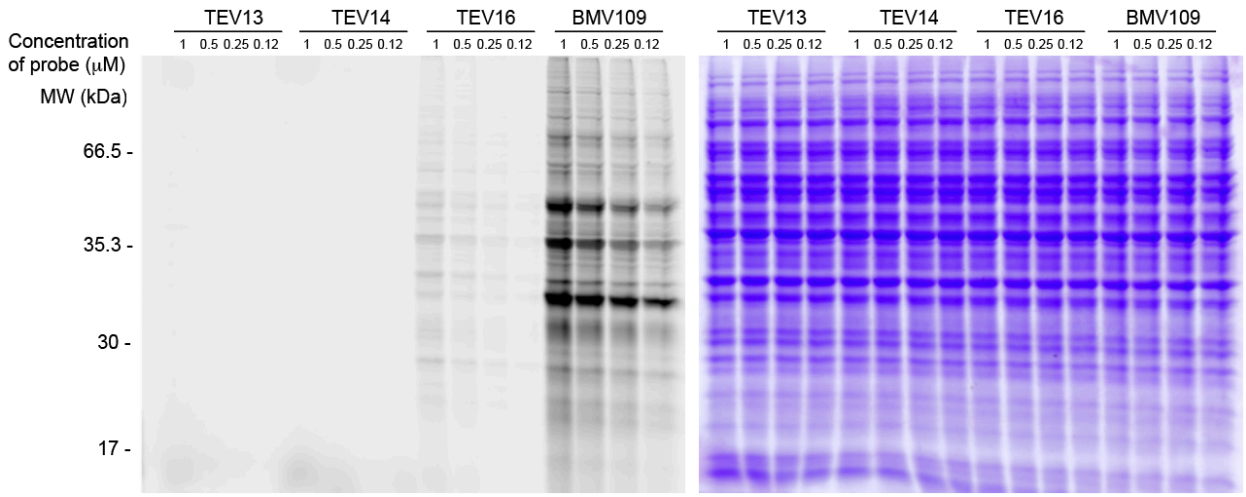

Supplementary Figure 12. Fluorescent labeling of total protein extracts from RAW cells at pH7.4 with various probes. Images of SDS-PAGE gels containing samples of the indicated total cellular lysates labeled for 1 hr with the indicated Cy5-ABPs. Samples were separated on SDS-PAGE gels followed by scanning for Cy5 fluorescence using a flatbed laser scanner (Left) and then stained with Coomassie brilliant blue (CBB; right) to visualize total protein loading. The probe BMV-109 is a general ABP for cysteine cathepsins that was included for reference.

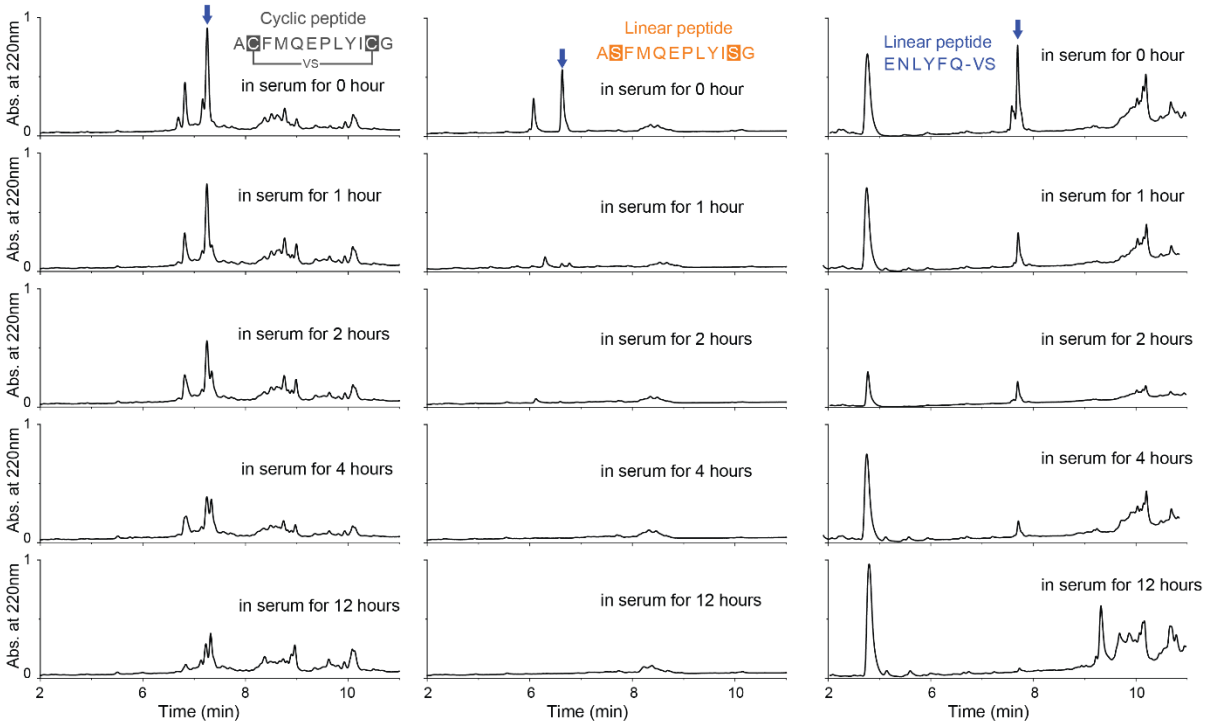

Supplementary Figure 13. Plasma stability of cyclic peptide TEV13, a linear version of the TEV13 peptide (H-ASFMQEPLYISG-NH_2, serine residues were used to replace cysteine residues to avoid the oxidative formation of cyclic peptide with disulfide bridge) and the linear vinyl sulfone peptide TEV16. Plots are HPLC traces of the extracted peptides after incubation in mouse plasma at 37 °C for the indicated times. The location of the peak corresponding to the intact original peptide is shown with a blue block arrow as determined by MS analysis.

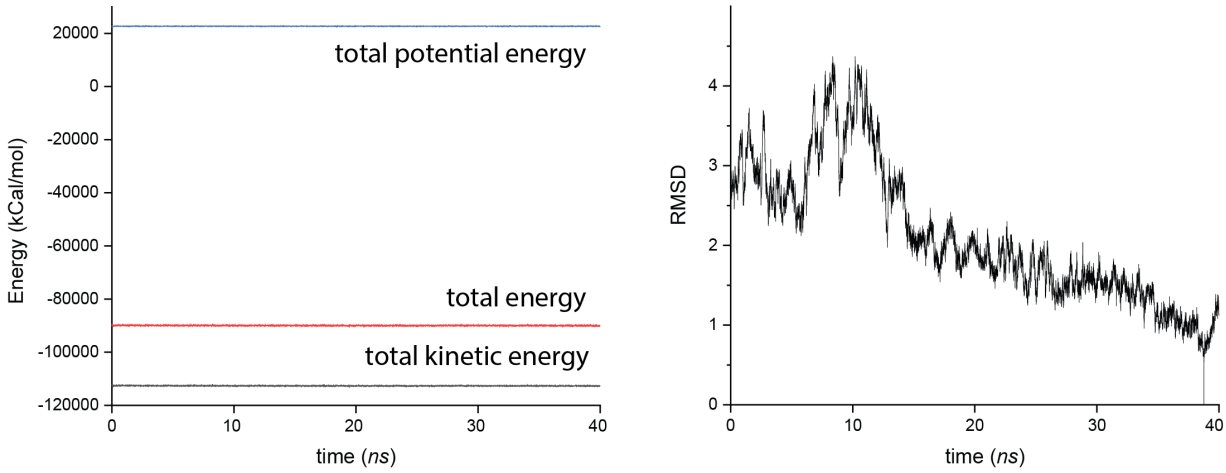

Supplementary Figure 14. Analysis of the Amber simulated structure of TEV13 complexed with the TEV protease. A) Total system energy of the 40 ns production simulation of the complex simulation in explicit TIP3P solvent models with ff14SB and gaff parameter sets. B) RMSD plot shows the evolution of the complex structure approaching the lowest energy conformation.